Lab on a Chip

Accepted Manuscript

ROYAL SOCIETY OF CHEMISTRY

www.rsc.org/loc

We present a micro-cytometer with excellent size accuracy, sensitivity and dynamic range and demonstrate its utility for accurate CD4 enumeration.

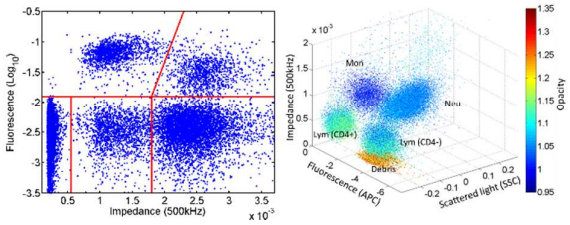

A sheath-less combined optical and impedance micro-cytometer

Daniel Spencer[1], Gregor Elliott[1] and Hywel Morgan*

Faculty of Physical Sciences and Engineering, and Institute for Life Sciences, University of Southampton, Southampton, Hampshire, SO17 1BJ, UK.

Abstract: We describe a sheath-less micro-cytometer that measures four different parameters, namely fluorescence, large angle side scatter and dual frequency electrical impedance (electrical volume and opacity). The cytometer was benchmarked using both size and fluorescent bead standards and demonstrates excellent size accuracy (CVs ≤2.1%), sensitivity and dynamic range (3.5 orders of magnitude) at sample flow rates of 80µL per minute. The cytometer is evaluated by analysing human blood, and we demonstrate a four part differential leukocyte assay for accurate CD4+ T-cell enumeration. The integration of impedance, fluorescence and side scatter into a single miniature cytometer platform provides the core information content of a classical cytometer in a highly compact, simple, portable and low cost format.

1. Introduction

Cytometry is widely used for the analysis of particles such as cells and beads, with application in areas as diverse as medicine, diagnostics [1-3] and oceanography [3-6]. Particle identification is usually performed with a combination of laser light scatter, laser induced fluorescence and electrical volume (Coulter) analysis [1,7], or in specialist systems using fast photography and image recognition [4,8,9]. Commercial cytometers are too large or costly for use anywhere other than in dedicated analysis laboratories. Therefore much work has been undertaken to develop micro-cytometers that would be smaller, cheaper and robust enough for use outside the lab [3,10,11]. Micro-cytometers have the potential to improve medical diagnosis by giving fast and accurate information of a wide variety of conditions. Small and compact cytometers are

[1] Both authors contributed equally to this work

*Corresponding author: hm@ecs.soton.ac.uk

also of interest in environmental science, for example in monitoring water to detect and classify alga [12].

Generally, particles are analysed using optical scatter; small angle forward scattered light (FSC) provides size information, whilst larger angle side scatter (SSC) gives information on internal structure and cell viability. Fluorescence detection provides further information on cell phenotype. For example, leukocytes are differentiated with fluorescent antibodies. Algal cells can be discriminated based on the spectral response of fluorescence from specific photosynthetic pigments in a particular species. Cytometers are widely used in haematology, where particle volume is measured using electrical (Coulter) methods [7].

Microfluidic Impedance Cytometry (MIC) has been developed to both count and discriminate cells. Multi-frequency impedance measurements are used to determine the dielectric properties of single particles [13-15]. Cells flow between two pairs of miniature electrodes which have an AC field applied across them. As the cell passes between the electrodes, the current path is disturbed and the change in current gives a single cell impedance signal. At low applied signal frequencies the technique provides accurate cell sizing where the impedance signal is proportional to cell volume. Higher frequency impedance measurements (1-5MHz in saline) give information on the cell membrane capacitance whilst much higher frequencies (>10MHz) probe the internal properties of the cell [13]. Two or more frequencies can be applied simultaneously to differentiate different cell types, for example white blood cell (wbc) subpopulations [14]. However, impedance cytometry cannot provide the information on cell phenotype that is obtained by labelling cells with fluorescent antibodies. As an analogue of fluorescent labelling, small dielectric particles can be used as impedance labels, but this technique can only identify a single subpopulation [16]. There is therefore a need to combine the simplicity and robustness of single cell impedance measurements with fluorescent interrogation methods in a single common microfluidic platform that is both

easy to manufacture and has comparable performance to conventional large-scale flow cytometers.

A variety of technologies have been demonstrated in the quest for a micro-cytometer that matches the performance of a conventional machine – for reviews see [10,11,13]. In early work Wolff *et al* [17] described a miniature fluorescence cell sorter fabricated in silicon, which used a waveguide to couple laser light into a channel and a microscope to collect fluorescence. Holmes *et al* [14] combined an impedance system with a lab based confocal microscope to measure fluorescence. Although the system could distinguish fluorescently labelled cells, it was very sensitive to particle position in the channel and consequently had a high coefficient of variation (CV) in fluorescence. Segerink *et al* described a simple cytometer that detects fluorescence [18] using an optical pickup from an HD-DVD player. They demonstrated that high precision mass manufactured optical components provides a cheap way of integrating optics. The system scans across the channel, therefore eliminating the need for fluidic focusing, but the fluidic throughput is limited to below 720pL/s, with a very low particle throughput of 1-2 beads per second.

Optical fibres are commonly used to deliver and collect light from micro-cytometers. For example, Wang *et al* [19] fabricated a cytometer that incorporated fibres coupled to waveguides to discriminate beads using scattered light, whilst Tung *et al* [20] used micro-groves for fibre alignment to detect fluorescently labelled yeast cells with PIN diodes and lock-in amplification.

Although most micro-cytometers are manufactured using planar lithography, devices have also been manufactured from milled plastic. Ligler *et al* have developed devices that use chevrons for particle focusing and optical fibres to deliver and collect light at the point of interrogation [21,22]. Neukammer and co-workers [23,24] manufactured a cytometer using a combination of micromachining and hot-embossing. The device used sheath flow and detected

fluorescence and scatter using optical fibres. They also included electrodes to measure impedance.

We recently demonstrated a micro-cytometer that measures optical and impedance parameters within a single chip [25]. Light was delivered and collected from the channel using integrated optical fibres and 1D sheath flow was used to focus particles. However, the cytometer suffered from several technological issues including misalignment of the optical fibres, incident light scatter from multiple interfaces and signals that strongly depended on particle position within the interrogation volume. All these problems degraded the CV of the measured particle populations. In many cytometers, the optical fibres are integral to the design. Inserting and aligning fibres is labour intensive, prone to error and does not provide for a modular system where chips can be easily replaced if they become contaminated or clogged. A modular cytometer that has interchangeable chips without integrated fibres would therefore be of significant advantage and could be used as part of a simple miniature system with a disposable consumable.

Nearly all micro-cytometers use some form of particle focusing for high quality (low CV) data. Typically, sheath flow is used to focus particles, and even in a micro-system this consumes of the order of 1mL per minute (see 21-24, 26-27). This imposes significant restriction on the technology for use at the point-of-care or for continuous monitoring. Sheath-less particle focusing techniques have also been reported. For example Hur *et al* used inertial forces to focus blood cells into 256 parallel microchannels [28]. High-speed imaging was used to analyse blood cells at a theoretical throughput of up to 1 million per second, however only 8000 cells were measured. The use of inertial focusing restricts simultaneous measurement of heterogeneous populations (RBCs had to be sphered prior to measurement). Curved microchannels and Dean forces have also been used to focus particles [29]. Acoustic, and dielectrophoretic focusing techniques have also been described [30,31]. However, in all these methods, the focusing force depends on particle size. The inertial migration force scales with

the square of particle radius, whilst acoustic and DEP forces scales with particle volume. In this paper we describe a micro-cytometer that does not require particle focusing. It measures particle impedance, fluorescence and large angle side scatter, with volumetric throughput, sensitivity and dynamic range comparable to a commercial flow cytometer. Signal processing is used to correct the impedance signal for particle position within the channel [32]. The optical excitation volume is designed to have uniform illumination and a thin metal screen is fabricated in the chip that minimises stray scattered light coupling into the collection optics. Light is coupled into the micro-channel using an integrated waveguide, and both fluorescence and SSC is measured using simple off-chip optics. The optical, fluidic and electrical connections are all designed so that the chip can be replaced easily in a small holder. Fluorescence sensitivity is evaluated using LinearFlow reference intensity beads. High accuracy impedance sizing is demonstrated using size calibration beads. The application of the technology to haematology is demonstrated by measuring different sub population of leukocytes, including CD14 monocytes and CD4+ T lymphocytes.

2. Experimental

The microfluidic chips (Figure 1) were made as described previously [14]. Platinum electrodes (30μm wide) were patterned onto glass substrates; channels and integrated optics were made from patterned SU8 with full wafer bonding in a vacuum bonder. Individual chips (25 x 10mm) were diced from the wafer. The fluidic channels had cross sectional dimensions of 30μm high and 80μm wide at the point of interrogation. A simple 1D hydrodynamic focusing region was included upstream from the measurement region. This was used to examine the fluorescence measurement performance with and without hydrodynamic focusing. To avoid any potential blockage with large particles, these channels are wider than previously used. The integrated optics, patterned in the SU8 layer, consisted of a waveguide running from the edge of the chip (Figure 1a) towards the edge of the channel. The waveguide was terminated with a cylindrical air lens (Figure 1b) patterned in SU8, which focused the light

into the channel. The optical path was designed using free-space optical calculations as described by Rosenauer *et al* [33]. The total optical path length from the chip edge to the centre of the channel is 5mm. The waveguide is 300μm wide at the edge of the chip and tapers to 60μm wide before the lens. The lens design is a double concave air lens (Figure 1b). In our previous design [25], light scatter from the waveguide and lens was a significant problem. In this design these elements were screened using the same metal layer that formed the electrodes. A small window was created for detection (Figure 1b).

Impedance detection requires separate electrical contacts for the top and bottom electrode pairs. The design shown in Figure 1 solves this problem and only requires connection to one side of the chip, with the top to bottom interconnection made individually using silver epoxy (see Figure S1 in the ESI).

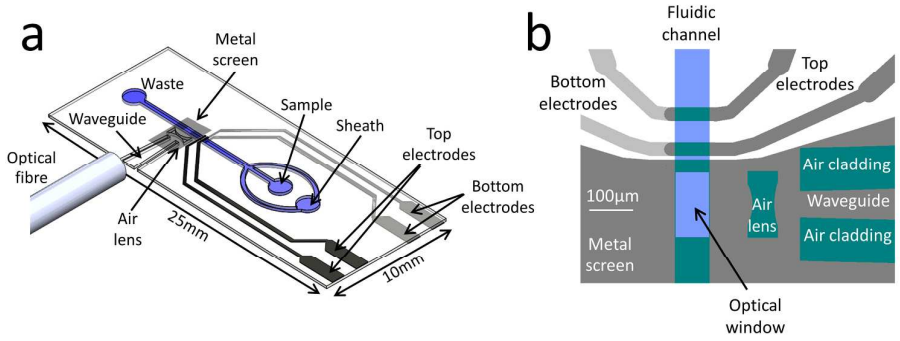

Figure 1. (a) Schematic diagram of the micro-cytometer chip showing showing the electrodes, the integrated waveguide that terminates on the edge of the chip, butt-coupled to an optical fibre for light delivery. Fluid inputs are shown for sample delivery and optional sheath flow. (b) shows a close up of the measurement region, with the lens, waveguide and impedance detection electrodes, together with the metal screen.

The chip was mounted in a plastic holder fabricated with a 3D printer (UP! Mini). The holder includes the fluidic and electrical connections with access ports for the fibre and detection optics (see Figure S2). Laser light is directed onto the side of the chip from a fibre, and an objective lens (x20), filter set and PMT collect the fluorescence and side scattered light. An image of the laser excitation light in the microfluidic channel, together with a cross sectional profile is also shown in

Figure S3. The image shows that the light is uniform across the channel and has a Gaussian profile along the direction of flow.

Single cell impedance was measured using an impedance spectroscope (Zurich instruments HF2IS). The electrical signal from the electrodes in the channel was measured with a trans-impedance amplifier (Zurich instruments HF2TA). The fluorescence signal from the PMT was plugged into the auxiliary port of the impedance spectroscope and sampled simultaneously with the electrical signal. Signals were sampled at 230ksps and post-processing was carried out using custom software written in Matlab. Signal processing was used to correct for variation in impedance with particle position in the channel [32].

Fluorescence performance was evaluated using AlignFlow beads (L14819), which are used to calibrate and align conventional flow cytometers. These beads are 6μm diameter, fluoresce at 660nm (when excited at 635nm), and have relative fluorescence intensities corresponding to 100%, 25%, 5%, 1.05%, 0.28%, 0.055%. Non-fluorescent 6μm diameter beads were also used.

Beads were suspended in phosphate buffered saline (PBS) at an approximate number density of 200 beads per microliter. The sample was loaded into a syringe and pushed through the chip at a constant flow rate with a syringe pump (Chemyx fusion 200). The device was design to operate without sheath flow, but for a full evaluation of the device, samples were also measured using a 1-D sheath flow of PBS. The ratio between the sample and sheath flow was varied, but the total flow rate was kept constant at 80μL/min for ease of comparison. In each case, the same sample was also analysed using a BD FACSAria, with the flow rate set to give similar particle throughput.

The sizing accuracy of the impedance micro-cytometer was evaluated using size calibration beads (3μm, 4.5μm, 6μm and 10μm in diameter from Polysciences), pumped through the chip at 80μL/min without sheath flow. For leukocyte measurements, blood was collected from a finger prick and pipetted directly into

EDTA tubes (MiniCollect 0.5mL K_3EDTA) which were placed on a roller to prevent aggregation. Leukocytes were labelled with fluorescent antibodies as follows. 50μL of blood was incubated with 10μL of CD14-APC or CD4-APC (Miltenyi) antibody for 10 minutes at room temperature (on a roller). Erythrocytes were subsequently removed by addition of 600μL of lysis solution (0.05% saponin 0.12% formic acid) and agitating for 6 seconds. The reaction was stopped with the addition of 265μL of quench solution (3%NaCL, 0.6%Na_2CO_3), as described previously [14]. Unbound antibody label was removed from the sample by centrifuging at 300g for 3 minutes, removing the supernatant and re-suspending the cells in PBS. This sample was measured with the microcytometer and a BD FACS Aria with a 633nm laser.

3. Results and Discussions

3.1 AlignFlow Beads

The micro-cytometer was designed to operate without sheath flow, but the BD FACSAria uses a constant pressure to provide sheath flow. The sample pressure is varied on a relative scale of 1-11, which effectively varies the diameter of the sample stream. These figures correspond to sample volumetric flow rates from approximately 10μL to 120μL/min. For the experiments, the flow rates on the FACSAria were set to approximately match the throughput on the micro-cytometer.

Figure 2 shows a section of a data stream showing simultaneous impedance and fluorescence data for AlignFlow fluorescent beads. Fig 2a-b shows raw un-processed signals for different beads (100%, 25%, 5%, 1.05%, 0.28%, 0.055%, 0% relative intensities) demonstrating excellent discrimination. The fluorescence signals from individual beads correlates with impedance signals. An example is shown in fig 2c-d, for a 1.05% intensity bead. The small 200μs offset in time arises from the displacement of the waveguide from the centre of the electrode pair by 245μm (see figure 1b). This offset was introduced to eliminate any potential effect of laser light on the impedance signals (through fluid heating).

The data in Fig 2 was obtained at a volumetric flow rate of 80μL/min, corresponding to a bead velocity of 0.8m/s.

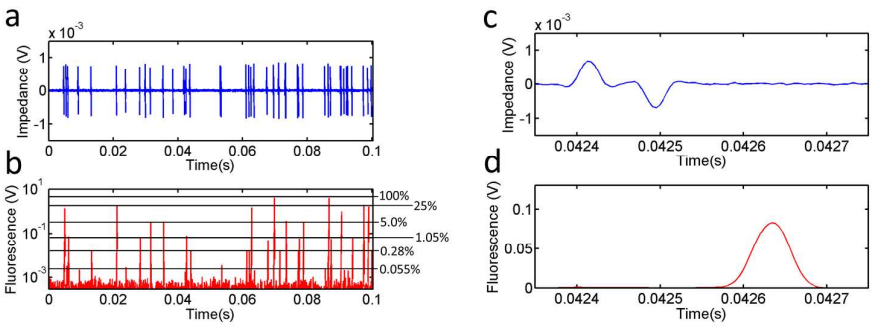

Figure 2 Raw data for 6μm AlignFlow beads. (a) shows impedance signals and (b) the corresponding fluorescence signals for six different bead intensities (b). Figures (c) and (d) show examples of impedance and fluorescence signals from a single particle, showing the very small offset in time between the two signals.

Figure 3 shows histograms for a single sample containing all different bead intensities measured on the micro-cytometer and the BD FACSAria. Impedance signals were used to trigger event detection on the micro-cytometer, and scatter on the FACSAria. The ratio of sheath to sample in the micro-cytometer was varied as shown in the figure, with the total volumetric flow kept constant at 80μL/min. The flow rate of the BD FACSAria was varied to give a similar sample throughput. The coefficient of variance (CV) and total particle counts for this data set are compared in table 1.

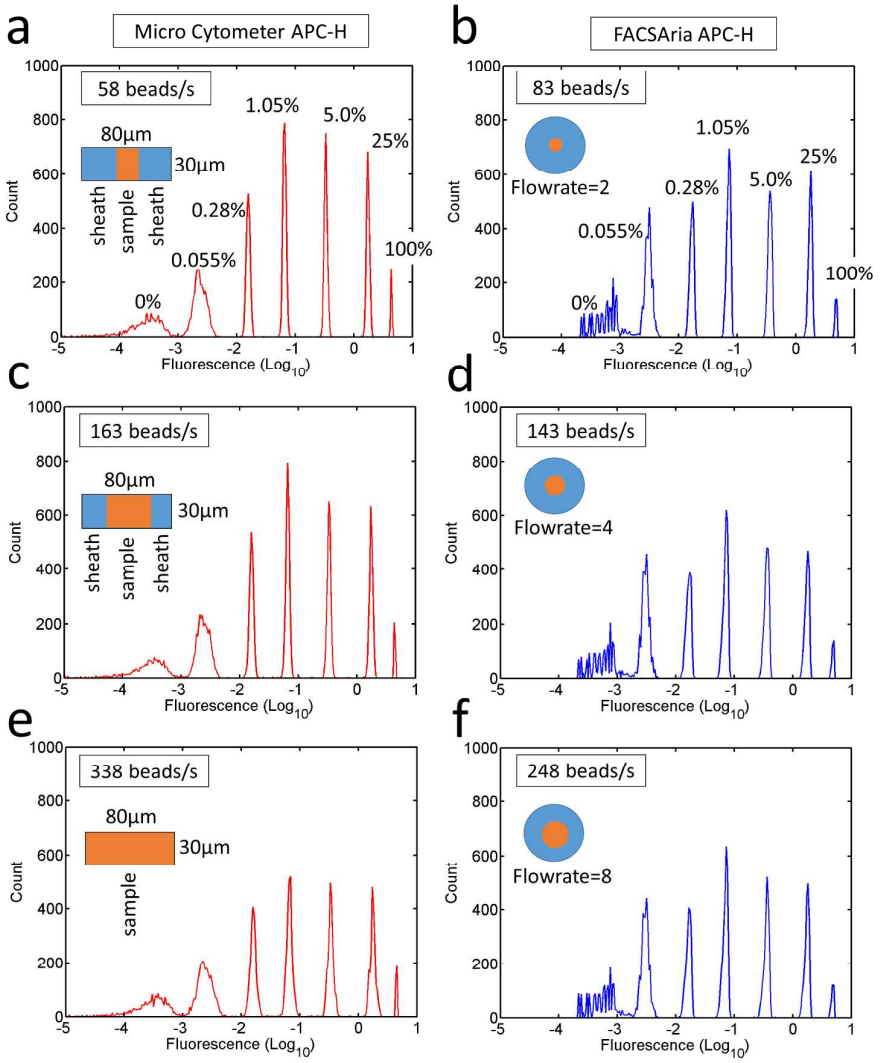

Figure 3 Fluorescence histograms of a suspension of all 7 bead intensities, measured on the micro-cytometer and the FACSAria. The micro-cytometer total sample rate was kept at 80µL/min with variable sheath to sample ratio. Flow rates were (a) sample=20µL/min, sheath =60µL/min, (c) sample=40µL/min, sheath=40µL/min, (e) sample=80µL/min, sheath=0µL/min. The FACSAria sample flow rate was: (b) 2/11 (approx. 20µL/min), (d) 4/11 (approx. 40µL/min), (f) 8/11(approx. 80µL/min); see inset images.

These histograms show that the lowest intensity fluorescence (0.055%) beads could be distinguished from the zero level on both systems, however, the dynamic range was insufficient to allow all 6 different intensities to be observed at the same time. Therefore the gain was set to allow the lowest intensity

particles to be detected, meaning that the 100% intensity particles saturated the detectors, (data not included in table 1).

Table 1 Comparison of CVs for fluorescent populations as measured by the micro-cytometer and FACSAria. Micro-cytometer measurements were taken at 80μL/min total flow with ratio of sheath to sample varied. The sample throughput on the FACSAria was similar to the micro cytometer. Refer to figure 3.

	Micro cytometer	FACS	Micro cytometer	FACS	Micro cytometer	FACS	Micro cytometer	FACS
Figure 3	(a)	(b)	(c)	(d)	(e)	(f)		
Sheath Flow Ratio	1:3		1:1		No sheath			
Measured throughput (beads/s)	58	83	163	143	338	248		
Fluorescence intensity (relative)	CV		CV		CV		Count (% total)	
100	-	-	-	-	-	-	2.30	2.21
25	6.04	6.49	6.70	7.80	10.7	8.3	14.4	14.0
5	6.00	7.32	6.87	8.41	10.6	9.35	15.8	15.6
1.05	6.20	7.27	7.04	8.62	11.0	9.17	19.1	18.7
0.28	7.61	7.62	8.15	9.47	11.5	9.78	15.1	14.4
0.055	24.5	20.2	24.3	20.0	27.9	20.2	21.0	22.3
0	46.0	36.0	44.3	36.2	46.3	36.8	12.3	12.6

Table 1 shows that for both systems, the CVs increase as the flow rate increases for all three flow rates. Importantly the CVs of the micro-cytometer are comparable to the FACSAria across all flow rates, as is the percentage count for each bead population. The data also shows that the optimum results for the micro-cytometer is obtained when using sheath flow to focus the particles. However, removing the sheath has very little influence on the CV data for

fluorescence, as seen by comparing the data in Figure 3(e) with (f), which shows a minor degradation in performance. This data should be compared with literature (e.g. Ligler [21, 22], Neukammer [23, 24] and Huang [26, 27]) where high volumetric sheath flows are required (typically of the order of 1mL/min) to give CVs comparable with reference cytometers.

High accuracy electrical volume measurement was demonstrated using a mixture of 3, 4.5, 6 and 10μm diameter beads suspended in PBS at a density of 1000 beads per μL. The bead suspension was flowed through the chip at 80μL/min with no sheath flow. In all cases the CV of the diameter (cube root of volume) is better than that quoted by the manufacturers (Table 2). This demonstrates the high accuracy particle sizing capability of the micro-cytometer even without sheath flow. Although forward scattered light is frequently used to measure particle size in flow cytometry, the dependence of Mie scatter with particle volume is non-linear, unlike impedance which scales linearly with particle volume. Additionally, it is technologically challenging to incorporate collection optics into micro-devices that can collect low-angle scattered light, although this has been done [34,35], but hydrodynamic particle focusing is required.

Table 2 Comparison of data for size calibration beads as given by the manufacturer and measured with the micro-cytometer.

	Manufacturer	**Measured**
Nominal size (um)	CV (%)	CV (%)
3	2.83	2.1
4.5	3.89	1.53
6	3.18	1.68
10	2.99	1.7

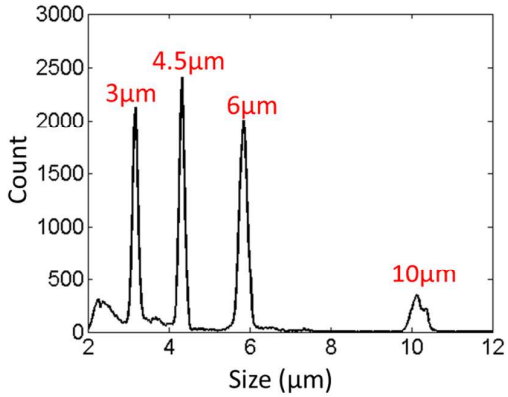

Figure 4 Histogram of electrically impedance size (cube root of impedance) for a mixture of calibration beads. The sample was measured at a volumetric flow rate of 80µL/min with no sheath flow.

As demonstrated by this data, the device operates exceptionally well without sheath flow. This brings significant advantages since the fluidics are much easier and robust (one inlet and outlet), and the system does not require additional large volumes of clean and sterile sheath liquid.

3.2 Leukocytes

The utility of the device for cell analysis was demonstrated by analysing CD14 labelled monocytes and CD4 T-lymphocytes with a combination of fluorescence, impedance and large angle scatter.

3-part White Blood Cell (wbc) differential: Simultaneous Impedance & fluorescence.

We have previously shown that impedance cytometry can perform a simple 3-part wbc differential based on measurement at two separate frequencies [14]. A low frequency signal (0.5MHz) provides information on cell size (volume) and discriminates smaller lymphocytes from granulocytes. Discrimination of monocytes from neutrophils requires a second higher frequency (2MHz) that measures cell membrane capacitance. Figure 5a shows a scatter plot for wbc differential measured on the micro-cytometer with electrical volume plotted on the x-axis and electrical opacity (ratio of high to low frequency) on the y-axis.

Opacity measures the cell membrane capacitance scaled with cell volume. The figure shows that the three major leukocyte populations can be distinguished solely on the basis of their electrical properties. A conventional FSC vs SSC plot measured on a FACSAria is shown in Figure 5b.

Additionally the monocytes were labelled with a fluorescent antibody (CD14-APC) and the fluorescence measured simultaneously with impedance. These fluorescent events are shown in red (Figure 5), with the histograms of fluorescence intensities shown in figure 5c-d. The data for the micro-cytometer was collected without sheath flow and compares favourably with the FACS data. The fine structures in the histogram of figure 5d is an artefact which arises due to quantisation of the data from the instrument and the subsequent histogram bins.

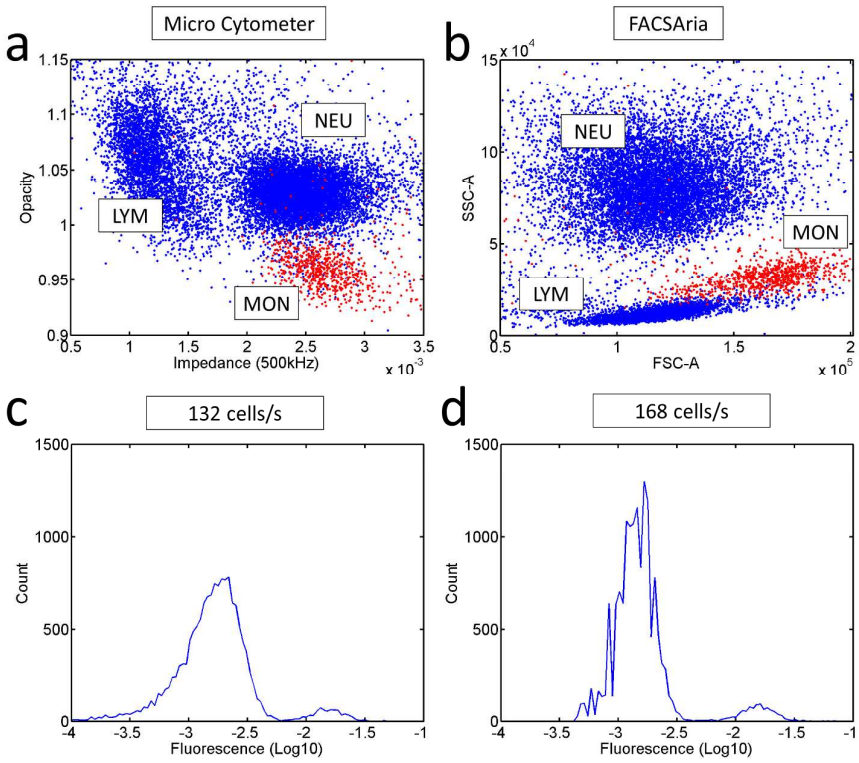

Figure 5. Scatter plots of a wbc differential measured on (a) the micro-cytometer and (b) the FACSAria (total number of events = 15,000). The three different cell sub-populations can be discriminated in both cases. The monocytes were labelled with fluorescent antibody (CD14-APC)

and the fluorescence histograms are shown in (c) and (d). The threshold level for fluorescent events (red) was set to -2.3.

The ability to further distinguish sub-populations was demonstrated by counting CD4+ T lymphocytes. An absolute CD4+ T-lymphocyte count is widely used to monitor the progression of HIV-AIDS. Initiation of antiretroviral treatment before the CD4 count falls below 200 cells/μL whole blood is recommended, and increased frequency of clinical monitoring is advised in patients with CD4 counts between 200 and 350 cells/μL. Either the absolute CD4 count or the CD4% can be used for diagnosis, but the absolute CD4 count is much preferred [36-38]. Disease is diagnosed by counting the T-cells that express the CD4 antigen on their surface. Monocytes also express the CD4 antigen, but at lower surface densities than the CD4+ T-cells [39]. It is important to distinguish the CD4+ T-lymphocytes from these other CD4 expressing cells to obtain accurate CD4 T-cell counts. In optical cytometry, a fluorescent label is used to identify the CD4+ cells and FSC and SSC discriminates monocytes from lymphocytes.

Figure 6(a) shows impedance-fluorescence scatter data for leukocytes labelled with CD4-APC. There are 5 classes of lymphocytes, of which approximately 50% express CD4 (Helper T-cells). This population is clearly identifiable in the figure. The monocytes also fluoresce but at a lower level, since these cells express five times fewer CD4 antibodies [39]. Impedance enables the lymphocytes to be distinguished from the larger neutrophils and monocytes. In optical cytometry FSC is used to size cells, but as shown in the FACSAria data (Figure 6b), this does not differentiate lymphocytes from neutrophils, which is normally done with SSC. However, the FSC signal is first used to gate the smaller particles and debris (Figure 6b) which overlaps with the lymphocyte population in SSC, as shown in the figure 6c. The final gates that are used to enumerate the leukocyte sub-populations is shown in Figure 6d. Finally, table 3 compares the counts and ratios (%) of the micro-cytometer with the FACSAria, and shows excellent agreement.

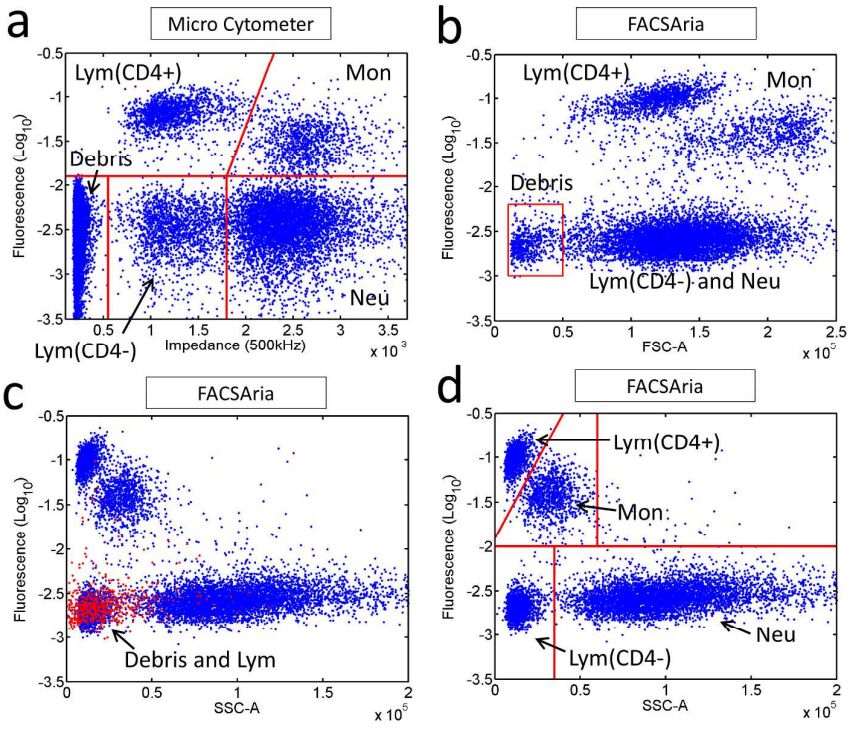

Figure 6 Four part differential of white blood cells measured on (a) micro-cytometer and (b) FACSAria. (b) to (d) demonstrates the process flow used to gate using FSC and SSC to determine the CD4 lymphocytes from the monocytes. Sample measured at a flow rate of 80µL/min (no sheath flow).

Table 3. WBC differential measured on the micro-cytometer and FACSAria

	micro-cytometer		FACSAria	
	Count	Relative %	Count	Relative %
Neutrophils	5580	55.8	5749	57.5
Monocytes	1116	11.2	1087	10.9
CD4+ Lymphocytes	1600	16.0	1476	14.8
CD4-Lymphocytes	1704	17.0	1688	16.9
Lymphocyte (CD4+/CD4-)	0.48		0.47	

The micro-cytometer can also measure side scatter, providing an additional parameter for cell identification (see Figure 2 ESI). Figure 7 shows a 3-D scatter plot for a different CD4 labelled leukocyte sample. This plot shows side scatter, fluorescence (APC) and low frequency impedance (particle volume), with the

impedance opacity (c.f. Figure 5) defining colour. The figure shows the same four wbc sub-populations, each identifiable according to one or more of the measured criteria.

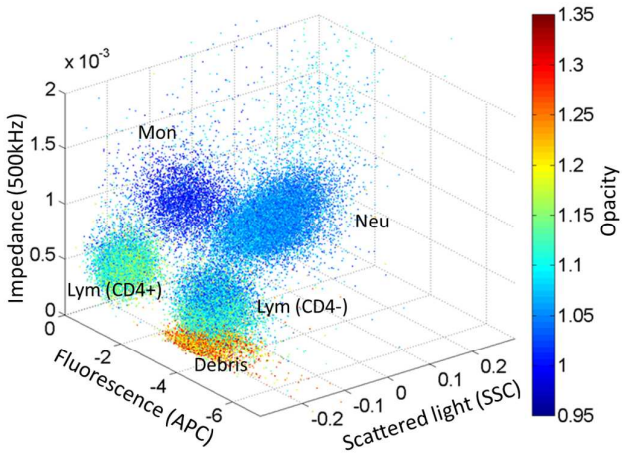

Figure 7. 3-D scatter plot for CD4-APC labelled wbcs for side scatter, fluorescence (natural log) and low-frequency impedance (electrical volume). Each data point is coloured according to electrical opacity. This multi-parameter plot demonstrates discrimination of the different cell sub-populations.

As shown by the bead and cell data, low-frequency impedance provides a very simple, yet accurate method for measuring particle volume. Unlike optical analysis, the method is easy to implement in a micro-device. Size or volume measurement is an essential parameter in flow-cytometric analysis of cells. However, measuring particle size using small angle forward scattered light is very difficult to implement in micro-systems due to the small angles involved and that fact that the incident light can couple into the detection optics, saturating the FSC detector. Goddin *et al* [34] used blackened baffles in the chip, and Watts *et al* [35] fabricated a notch in the delivery optics to prevent incident light entering the FSC detection waveguide. However in both cases the SNR was very low, and the CV in the FSC signal was much poorer than measurements using conventional cytometers. Additionally, both devices required sheath flow to centre particles in the channel. By contrast, impedance is very simple and can size particles with very high accuracy, for example with CVs of 1.5-2.1%, better than manufacturer's quoted data (2.8-3.9%) and in the absence of sheath flow. Our micro-cytometer has similar performance to the FACSAria at volumetric flow

rates of up to 80μL/min with cell counts of hundreds of cells per second despite our comparatively low sampling rate. The volumetric throughput is higher than comparable miniature cytometers which mostly operate around 10μL-20μL/min [21-24], but similar to conventional cytometers (typical sample flow rates of 100μL/min). Our particle throughput is up to 1000 per second. Although this is lower than the quoted maximum throughput of many bench-top cytometers, there is always a trade-off between speed and accuracy. At high throughputs (e.g. 10,000 per second) coincidence becomes a problem. Simmonet and Groisman were the first to demonstrate a high speed fluorescence-based micro cytometer with a maximum throughput of 17,000 per second [40]. CV's were comparable to a commercial cytometer, however the device utilised a complex 3D hydrodynamic focusing architecture which required precisely balanced pressure driven flows for each of the four inlets. To achieve maximum throughput the bead concentration was very high (~$2.8x10^8$ per mL) and the cytometer was not sensitive enough to measure fluorescently marked live cells.

Throughput can be increased in many ways. The sampling rate of the electronics hardware places an upper bound on the flow-rate. Conventional cytometers sample at around 10Msps, whereas our electronics is limited to 0.23Msps. Utilising high speed electronics would increase the maximum flow-rate by at least one order of magnitude (up to the Nyquist limit). Fundamentally, throughput is limited by particle coincidence, which for a random distribution of particles is defined by Poisson statistics. Particle concentration could be increased but to avoid coincidence, particles need to be laterally ordered using techniques such as inertial focussing [41]. Alternatively, throughput could be increased by using multiple parallel streams [42].

4. Conclusions

A high accuracy modular micro-cytometer that incorporates impedance, side scatter and fluorescence has been described. The device was benchmarked against a BD FACSAria using fluorescent and size calibration beads. Application to haematology analysis was demonstrated by enumerating antibody labelled white blood cells. A combination of multi-frequency impedance, SSC and

fluorescence provides all the primary metrics required for high speed single cell analysis. Since the cytometer is sheath-less, all that is required is a single syringe pump for the sample. The system is modular, with easy optical, fluidic and electric interconnects to the chip. Impedance-based particle sizing outperforms particle sizing from on-chip FSC, with excellent CVs ≤2.1%. The device also has a large dynamic range in fluorescence with CVs comparable to a BD FACSAria at the same high sample flowrate of 80µL per minute. The integration of impedance, fluorescence and side scatter into a single miniature cytometer platform provides the core information content of a classical cytometer in a highly compact, simple, portable and low cost format. A CD4 lymphocyte count from human blood demonstrates that this device could be used for haematology analysis away from a centralised lab.

Acknowledgements

The authors acknowledge funding from the European Union (DIMID project) and the Royal Society.

References

[1] HM Shapiro, *Practical Flow Cytometry*, 2003, John Wiley & Sons, Hoboken, New Jersey.
[2] RC Sobti, *Advanced flow cytometry: applications in biological research*, 2003, Kluwer Academic Publishers, Dordrecht, The Netherlands.
[3] JS Kim and FS Ligler, *The Microflow Cytometer,* 2010, Pan Stanford Publishing, Singapore.
[4] L Campbell, RJ Olson, HM Sosik, A Abraham, DW Henrichs, CJ Hyatt and EJ Buskey, *First Harmful Dinophysis (Dinophyceae, Dinophysiales) Bloom in the U.S. Is Revealed by Automated Imaging Flow Cytometry*, J Phycol, 2010, **46**, 66-75.
[5] M Thyssen, GA Tarran, MV Zubkov, RJ Holland, G Gregori, PH Burkill and M Denis, *The emergence of automated high-frequency flow cytometry: revealing temporal and spatial phytoplankton variability*, J Plankton Res, 2008, **30**, 333-43.
[6] RJ Olson, A Shalapyonok, HM Sosik, *An automated submersible flow cytometer for analyzing pico- and nanophytoplankton: FlowCytobot*, Deep-Sea Res Pt I, 2003, **50**, 301-15.
[7] WH Coulter, *High Speed Automatic Blood Cell Counter and Cell Size Analyser*, Proc Natl Electron Conf, 1956, **12**, 1034–1040.
[8] RJ Olson and HM Sosik, *A submersible imaging-in-flow instrument to analyze nano- and microplankton: Imaging FlowCytobot*, Limnol Oceanogr-Meth, 2007, **5**, 195-203.
[9] K Goda, A Ayazi, DR Gossett, J Sadasivam, CK Lonappan, E Sollier, AM Fard, SC Hur, J Adam, C Murray, C Wang, N Brackbill, D Di Carlo, and B Jalali, *High-throughput single-microparticle imaging flow analyser*, PNAS, 2012, 1204718109.
[10] DA Ateya, JS Erickson, PB Howell, LR Hilliard, JP Golden and FS Ligler, *The good, the bad, and the tiny: a review of microflow cytometry*, Anal Bioanal Chem, 2008, **391**, 1485-98.
[11] SH Cho, JM Godin, CH Chen, W Qiao, H Lee, YH Lo, *Review Article: Recent advancements in optofluidic flow cytometer*, Biomicrofluidics, 2010, **4**, 043001.
[12] N Hashemi, JS Erickson, JP Golden, FS Ligler, *Optofluidic characterization of marine algae using a microflow cytometer*, Biomicrofluidics, 2011, **5**, 032009.
[13] T Sun, H Morgan, *Single-cell microfluidic impedance cytometry: a review*, Microfluid Nanofluid, 2010, **8**, 423-43.
[14] D Holmes, D Pettigrew, CH Reccius, JD Gwyer, C van Berkel, J Holloway, DE Davies and H Morgan, *Leukocyte analysis and differentiation using high speed microfluidic single cell impedance cytometry*, Lab on a Chip, 2009, **9** 2881-9.
[15] S Gawad, L Schild and Ph Renaud, *Micromachined impedance spectroscopy flow cytometer for cell analysis and particle sizing*, Lab Chip, 2001, **1**, 76-82.
[16] D Holmes and H Morgan, *Single Cell Impedance Cytometry for Identification and Counting of CD4 T-Cells in Human Blood Using Impedance Labels*, Anal Chem, 2010, **82**, 1455-61.
[17] A Wolff, IR Perch-Nielsen, UD Larsen, P Friis, G Goranovic, CR Poulsen, JP Kutter and P Telleman, *Integrating advanced functionality in a microfabricated high-throughput fluorescent-activated cell sorter*, Lab Chip, 2003, **3**, 22-7.
[18] LI Segerink, MJ Koster, AJ Sprenkels and A van den Berg, *A low-cost 2D fluorescence detection system for µm sized beads on-chip*, Lab Chip, 2012, **12** 1780-3.
[19] Z Wang, J El-Ali, M Engelund, T Gotsaed, IR Perch-Nielsen, KB Mogensen, D Snakenborg, JP Kuter and A Wolff, *Measurements of scattered light on a microchip flow cytometer with integrated polymer based optical elements*, Lab Chip, 2004, **4**, 372-7.
[20] YC Tung, M Zhang, CT Lin, K Kurabayashi and SJ Skerlos, *PDMS-based opto-fluidic micro flow cytometer with two-color, multi-angle fluorescence detection capability using PIN photodiodes*, Sens Actuators B, 2004, **98**, 356-67.

[21] AL Thangawng, JS Kim, JP Golden, GP Anderson, KL Robertson, V Low and FS Ligler, *A hard microflow cytometer using groove-generated sheath flow for multiplexed bead and cell assays*, Anal Bioanal Chem, 2010, **398**, 1871-81.
[22] LC Shriver-Lake, J Golden, L Bracaglia and FS Ligler, *Simultaneous assay for ten bacteria and toxins in spiked clinical samples using a microflow cytometer*, Anal Bioanal Chem, 2013, **405**, 5611-5614.
[23] A Kummrow, J Theisen, M Frankowski, A Tuchscheerer, H Yildirim, K Brattke, M Schmidt and J Neukammer, *Microfluidic structures for flow cytometric analysis of hydrodynamically focussed blood cells fabricated by ultraprecision micromachining*, Lab on a Chip, 2009, **9**, 972-81.
[24] M Frankowski, J Theisen, A Kummrow, P Simon, H Ragusch, N Bock, M Schmidt and J Neukammer, *Microflow cytometers with integrated hydrodynamic focussing*, Sensors, 2013, **13**, 4674-4693.
[25] D Barat, D Spencer, G Benazzi, MC Mowlem and H Morgan, *Simultaneous high speed optical and impedance analysis of single particles with a microfluidic cytometer*, Lab Chip, 2012, **12**, 118-26.
[26] X Mao, AA Nawaz, SCS Lin, MI Lapsley, Y Zhao, JP McCoy, WS El-Deiry and TJ Huang, *An integrated, multiparametric flow cytometry chip using "microfluidic drifting" based three-dimensional hydrodynamic focusing* Biomicrofluidics, 2012, **6**, 024113.
[27] AA Nawaz, X Zhang, X Mao, J Rufo, SCS Lin, F Guo, Y Zhao, M Lapsley, P Li, JP McCoy, SJ Levine and TJ Huang, *Sub-micrometer-precision, three-dimensional (3D) hydrodynamic focussing via "microfluidic drifting"*, Lab Chip, 2014, **14**, 415.
[28] SC Hur, HT Kwong Tse and D Di Carlo, *Sheathless inertial cell ordering for extreme throughput flow cytometry*, Lab Chip, 2010, **10**, 274-280.
[29] AAS Bhagat, SS Kuntaegowdanahalli, N Kaval, CJ Seliskar and I Papautsky, *Inertial microfluidics for sheath-less high-throughput flow cytometry*, Biomed Microdevices, 2010, **12**, 187-195.
[30] Y Chen, AA Nawaz, Y Zhao, PH Huang, JP McCoy, SJ. Levine, L Wang and TJ Huang, *Standing surface acoustic wave (SSAW)-based microfluidic cytometer*, Lab Chip, 2014, **14**, 916-923.
[31] D Holmes, H Morgan and NG Green, *High throughput particle analysis: Combining dielectrophoretic particle focussing with confocal optical detection*, Biosens. Bioelectron, 2006, **21**, 1621-1630.
[32] D Spencer and H Morgan, *Positional dependence of particles in microfludic impedance cytometry*, Lab Chip, 2011, **11**, 1234-9.
[33] M Rosenauer, W Buchegger, I Finoulst, P Verhaert and M Vellekoop, *Miniaturized flow cytometer with 3D hydrodynamic particle focusing and integrated optical elements applying silicon photodiodes*, Microfluid Nanofluid, 2011, **10**, 761-71.
[34] J Godin and YH Lo, *Two-parameter angular light scatter collection for microfluidic flow cytometry by unique waveguide structures*, 2010, Biomed opt express, 2010, 1, **5**, 1472-1479.
[35] BR Watts, Z Zhang, CQ Xu, X Cao and M Lin, *A method for detecting forward scattering signals on-chip with a photonic-microfluidic integrated device*, Biomed opt express, 2013, **4**, 7, 1051-1060.
[36] *Laboratory Guidelines for enumerating CD4 T-Lymphocytes in the context of HIV/AIDS*. WHO, June, 2007, ISBN 9789290222989.
[37] Dunn DT, *HIV Paediatric Prognostic Markers Collaborative Study: Use of total lymphocyte count for informing when to start antiretroviral therapy in HIV-infected children: a meta-analysis of longitudinal data*, Lancet, 2005, **366**, 1868–1874.
[38] *Revised classification system for HIV infection in children less than 13 years of age; Official authorized addenda: human immunodeficiency virus infection codes and official guidelines for coding and reporting* ICD-9-CM. MMWR 1994, 43, RR-12.

[39] B Lee, M Sharron, LJ Montaner, D Weissman and RW Doms, *Quantification of CD4, CCR5, and CXCR4 levels on lymphocyte subsets, dendritic cells, and differentially conditioned monocyte-derived macrophages*, Proc. Natl. Acad SciPNAS, 1999, **96**, 5215-5220.
[40] C Simonnet and A Groisman, *High-Throughput and High-Resolution Flow Cytometry in Molded Microfluidic Devices*, Anal Chem, 2006, **76**, 5653-5663.
[41] D Di Carlo, D Irimia, RG Tompkins and M Toner*, Continuous inertial focusing, ordering, and separation of particles in microchannels*, PNAS, 2007, **104**, 48, 18892-18897.
[42] ME Piyasena, PPA Suthanthiraraj, RW Applegate, AM Goumas, TA Woods, GP Lopez and SW Graves, *Multinode acoustic focussing for parallel flow cytometry*, Anal Chem, 2012, **84**, 1831-1839.